Biomacromolecules

Article

Tough Magnetic Chitosan Hydrogel Nanocomposites for Remotely Stimulated Drug Release

Yongliang Wang, Baoqiang Li, Feng Xu, Zhidong Han, Daqing Wei, Dechang Jia, and Yu Zhou

Biomacromolecules, **Just Accepted Manuscript** • DOI: 10.1021/acs.biomac.8b00636 • Publication Date (Web): 11 Jul 2018

Tough Magnetic Chitosan Hydrogel Nanocomposites for Remotely Stimulated Drug Release

Yongliang Wang,[1] *Baoqiang Li,*[*,2,3] *Feng Xu,*[4] *Zhidong Han,*[1] *Daqing Wei,*[2] *Dechang Jia,*[2] *and Yu Zhou*[2]

1 College of Materials Science and Engineering, Harbin University of Science and Technology, Harbin 150040, China

2 Institute for Advanced Ceramics, State Key Laboratory of Urban Water Resource and Environment, Harbin Institute of Technology, Harbin 150001, China.

3 Key Laboratory of Advanced Structural-Functional Integration Materials & Green Manufacturing Technology, Harbin Institute of Technology, Harbin, 150001, China

4 The Key Laboratory of Biomedical Information Engineering of Ministry of Education, Biomedical Engineering and Biomechanics Center, Xi'an Jiaotong University, Xi'an 710049, China.

ABSTRACT

As one of important biomaterials for localized drug delivery system, chitosan hydrogel still exist several challenges, including poor mechanical properties, passive drug release behavior and lack of remote stimuli response. To address these challenges, a facile *in-situ* hybridization method was reported for fabricate tough magnetic chitosan hydrogel (MCH), which remotely switched drug release from passive release to pulsatile release under a low frequency alternating magnetic field (LAMF). The *in-situ* hybridization method avoided the aggregation of magnetic nanoparticles (MNPs) in hydrogel, which simultaneously brings 416 % and 265 % increase in strength and elastic modulus, respectively. The mechanical property enhancement was contributed by the physical crosslinking of *in-situ* synthesized MNPs. When a LAMF with 15min ON-15min OFF cycles was applied to MCH, the fraction release showed zigzag shape and pulsatile release behavior with quick response. The cumulative release and fraction release of drug from MCH were improved by 67.2 % and 31.9 %, respectively. MTT results and cell morphology indicated that the MCH have excellent biocompatibility and no acute adverse effect on MG-63 cells. The developed tough MCH system holds great potential for applications in smart drug release system with noninvasive characteristics and magnetic field stimulated drug release behavior.

KEYWORDS: chitosan; magnetic hydrogel; remote stimulation; smart drug delivery;

Introduction

Hydrogels have attracted increasing attention as drug release carriers, since they can provide more options for drug administration (*e.g.*, implantation) and achieve designed drug release behaviors in target tissues with improved bioavailability, drug efficacy and tolerance, and

reduced toxicity.[1] However, most of hydrogel carriers release drugs in a passive manner (*e.g.*, via diffusion, matrix degradation) with limited control over the drug release behavior.[2] External stimuli-sensitive hydrogels hold great potential to control drug release behavior by changing gel structure in responsive to specific stimulations, such as pH and temperature.[3] Among various hydrogels, chitosan hydrogel as one of natural polysaccharide hydrogels has unique characteristics (*e.g.*, biodegradability, plenty of active groups ($-NH_2$ and -OH)), which make it excellent candidate as drug delivery carriers. [4,5]

Various stimulated drug release strategies have been developed based on chitosan hydrogel,[6] such as pH-sensitive stimulation,[7] thermo-sensitive stimulation,[8] enzyme-sensitive stimulation[9] and near infrared or magnetic field heating thermo-sensitive polymer synergistic stimulation.[10] For instance, many pH-sensitive chitosan hydrogels have been developed, such as chitosan/glutaraldehyde, chitosan/genipin, chitosan/sodium tripolyphosphate and chitosan/alginate,[11] due to the special solubility properties of chitosan (easily dissolved at low pH and significant insolubility at neutral pH). Although these systems have provided the possibility to control drug release from chitosan hydrogel, they are associated with several limitations. For instance, the response time of existing pH-sensitive or thermo-sensitive hydrogels is too long (several hours). Besides, it is difficult to alter pH or temperature in human body due to the relatively stable pH, temperature and enzyme condition of human body. It is also challenging for these methods to localize these stimulations to the target area and control the drug release remotely, which are important for noninvasiveness without disturbing the biological environment. Finally, the mechanical properties of natural biodegradable hydrogels are weak and fragile nature with strength less than 60 kPa limiting their application as implantable localized

drug release system.[12] Therefore, there is still an unmet need for a tough and durable physical crosslinked drug release hydrogel with quick response and remote controllability.[13]

Magnetic hydrogels or ferrogel (*i.e.*, hydrogels containing magnetic nanoparticles (MNPs)) have been widely used in biomedical applications, such as tissue engineering,[14] soft actuators,[15] magnetic resonance imaging,[16] hyperthermia therapy and drug release system.[17] They offer several advantages compared to other stimulation-sensitive drug release systems, including rapid response, remotely controlled movement, noninvasive heat generation and easy localization of physical cue.[18,19] MNPs embedded in thermo-sensitive hydrogel has been applied to modulate drug release driven by matrix response to temperature changing induced by heat effect of high frequency alternating magnetic field.[20,21] However, the drug release behavior was achieved by converting high frequency alternating magnetic field into heat to induce volume change or phase change of ferrogel. The temperature increase may disturb the drug release mechanism and involve the issue of potential risk for biological tissue.

Many existing magnetic sensitive drug carriers are not biodegradable and may induce local inflammation. Several papers have reported about magnetic chitosan beads or magnetic alginates beads which were obtained by mixture of MNPs and chitosan or alginate, in which MNPs were chosen as magnetic-sensitive moiety due to its high compatibility.[22,23] Besides, simple mixture of MNPs and chitosan arises the problem of aggregation of MNPs in hydrogel and cell toxicity due to the unmodified MNPs released from hydrogel.[19,24,25] MNPs aggregation may also result in the consequent loss of superparamagnetic behavior of MNPs due to their size dependent character and the non-uniform deformation of hydrogel in the gradient magnetic field which may disturb the drug release profile.[26,27] It is thus critical to prevent the MNPs from aggregating. However, it

is still challenging to achieve uniform MNPs distribution in hydrogel through a simple blending. Besides, MCH has not been applied for controlled drug release yet.

To address the above mentioned challenges, we fabricated magnetic chitosan hydrogels (MCH) by *in-situ* synthesis of MNPs during chitosan gelation to achieve magnetic response and reinforced mechanical properties simultaneously. We directly controlled the drug release behavior in a remote manner by using low frequency alternating magnetic field (LAMF), which also avoided the potential adverse heat effect. Both hydrophilic drug adriamycin and hydrophobic drug rifampicin were used to investigate the passive drug release in absence of magnetic field and pulsed drug release from MCH remotely stimulated by ON-OFF low frequency alternating magnetic field. The strong and smart magnetic nanocomposite hydrogels served as an implantable drug carrier for remotely stimulated drug delivery system.

Experimental Section

Synthesis of Magnetic Chitosan Hydrogels. Schematic presentation of the principle of *in-situ* hybridization for MCH was shown in **Figure 1**. Briefly, 4 g chitosan was dissolved in 100 mL acetic acid solution (2 %, v/v) and chitosan solution (4 %, wt/wt) was obtained. 10 mL of magnetite precursor containing 7 mmol iron(III) and 3.5 mmol iron(II) was added into the chitosan solution and stirred for 2 h to obtain a homogeneous solution. The mixture was soaked in NaOH solution (1.25 mol/L) for 4 h, and OH^- diffused into the mixture. The OH^- ions induced deprotonation of chitosan and crystallization of magnetite, and MCH was obtained. Finally, deionized water was used to rinse the MCH to neutral. A chelation effect existed between chitosan and iron ions (Figure 1a), which ensured homogeneous dispersion of MNPs in chitosan hydrogel (Figure 1b) and the oxidation of *in-situ* synthesized MNPs was also prevented.

Moreover, a weak interaction was formed between chitosan and MNPs after hybridization, which enhanced the mechanical properties of MCH and endowed the MNPs with an *in-situ* chitosan layer.[34]

Distribution of Magnetite Nanoparticles in MCH. The microstructure of MCH was checked using an Environmental Scanning Electron Microscope (ESEM, Quanta 2000FEI). Samples were loaded onto sample platform and dipped in liquid nitrogen slush. After that, the samples were directly investigated in ESEM at an accelerating voltage of 12.5 kV. Transmission Electron Microscopy (FEI Tecnai F20 G2) was used to assess the distributions of MNPs in MCH as well as interface between chitosan and MNPs.

Determination of Mechanical Properties of MCH. The mechanical properties of MCH with different concentrations of magnetite nanoparticles (0, 5 wt.%, 10 wt.%, 15 wt.% and 20 wt.%) were tested on a Texture Analyzer TA. XT plus (Stable Micro System, UK) in MARMALADE mode.[35] The probe (P/0.5) with 5 kg load cell was compressed into the sample to a depth of 15 mm at the test-speed of 1 mm/s. All measurements were performed 3 times and the parameters calculated as mean values ± standard deviation.

Drug Release Behavior of MCH in Magnetic Field. Adriamycin (ADM) and rifampicin (RFP) were used as water soluble and insoluble model drugs for drug release demonstration of MCH. The incorporation of ADM and RFP into hydrogel was performed via post-loading. The MCH had a disc shape with diameter of 25 mm and height of 5 mm. The MCH were soaked in ADM or RFP solution (20 mg/mL) for 72 h at 25 °C, and then washed with PBS for 10 min. The solvent of drug solution was PBS (pH = 7.4) and the MCH reached swelling equilibrium at 4 h during drug-loading. The drug-loaded MCH were dissolved in 2 wt.% acetic acid and the drug

loading content was determined by a UV-vis spectrometer (Avanta Ultra Z). Finally, the drug loaded MCH was putted in 100 mL PBS solution to investigate the release behavior. At specific intervals (15 min for water soluble drug or 1 h for insoluble drug), an aliquot release medium (3 mL) was withdrawn from 100 mL and replaced with 3 mL fresh PBS. The cumulative release of ADM and RFP were determined by UV-vis spectrometer at 484 nm and 254 nm.

The schematic of setting for magnetic remotely stimulated drug release from MCH in presence of a low frequency alternating magnetic field (LAMF) is shown in Figure 1d. The drug loaded MCH was placed in 100 mL PBS and LAMF with strength of 0.4 T was provided by one pair of rotated permanent magnets with frequency of 2 Hz. The period of LAMF "ON" were 15 min and 1 h for ADM and RFP, respectively. The setting was removed when LAMF was "OFF". The drug release fraction from MCH was measured by UV-vis. Paired samples *t* test was used to identify with significant differences ($P < 0.05$) between LAMF drug release and passive drug release. All statistical analyses were performed with the software SPSS v17.0.

Cytotoxicity of *in-situ* Synthesized MNPs Released from MCH. In order to obtain the cytotoxicity of *in-situ* synthesized MNPs released from MCH, MCH was dissolved in acetic acid solution and centrifugated at 5000×g for 15min to remove the indissoluble content, then the MNPs were obtained by centrifugation the supernatant at 12000×g for 15min. The human osteosarcoma cells (MG-63), at a density of 4×10^4 cells/mL, were cultured in McCoy's 5A medium containing 10 % fetal bovine serum (FBS) in a CO_2 incubator. The CO_2 incubator maintained at 5 % CO_2 at 37 °C for 24 h, and then the cell medium was replaced by medium containing MNPs for another 48 h. The doses of MNPs were set as 50, 100, 150 and 200 mg/L. The viability of MG-63 cells was determined by the 3-(4,5-dimethylthiazol-2-yl)-2,5-diphenyltertrazolium bromide (MTT) test. The cells, cultured in cell medium containing different

concentrations of MNPs, were washed three times carefully with PBS to remove the extracellular MNPs. Cell Proliferation Kit (Sigma-aldrich Co.) was used for cytotoxicity investigation according to the manufacturer's protocol. 10 μL of MTT solution was added and incubated for 4 h, and then formazan crystals were dissolved in 100μL of solubilization buffer. The percent cell viability was calculated using an ELISA plate reader at 570 nm.

Morphologies of MNPs in MG-63 Cells. The morphology of MG-63 with internalized MNPs was investigated by Transmission Electron Microscopy (H-7650, Hitachi) after the cells were embedded and treated by ultra-thin cutting. Briefly, MG-63 cells were fixed in glutaraldehyde (2.5 vol.%) for 2 h and washed with PBS solution for three times. Then the cells were fixed in osmium tetroxide for 2 h and washed with PBS for three times. After that, the samples were dehydrated in ascending concentrations of ethanol (50, 70, 80, 90, 95 and 100 %, 15 min each). The dehydrated cells were embedded in Spurr resin. Finally, the embedded cells were treated by ultra-thin cutting for TEM investigation.

Results and Discussion

Tough Magnetic Chitosan Hydrogels via *in situ* Hybridization

The MCH was synthesized via *in-situ* hybridization. As can be seen from **Figure 1**a, a chelation effect existed between amino groups of chitosan and iron ions (CS-NH_2-Fe(III,II)), which induced homogenous distribution of iron ions. When the above mixture encountered OH^-, the OH^- ions induced deprotonation of chitosan and crystallization of magnetite (Figure 1b). Due to the uniform dispersion of iron ions which were chelated by amino groups of chitosan, the aggregation of MNPs was avoided.

Morphologies of Magnetic Chitosan Hydrogels.

To evaluate the particle size, distribution of *in-situ* synthesized MNPs and the interface between MNPs and hydrogel, we investigated the morphology of MCH using ESEM and TEM (**Figure 2**). Sharp freezing by liquid nitrogen makes it possible to observe the distribution of MNPs in MCH with plenty of water by ESEM without sample distortion. No aggregation of MNPs was detected in Figure 2a, which proved the homogenous distribution of MNPs in MCH. The morphology of MNPs with nanosize was shown in Figure 2b and c. We observed that the MNPs with diameter of ~9 nm (Figure 2d) were uniformly dispersed in physical crosslinked hydrogel and there was no significant aggregation. However, some MNPs aggregations appeared in magnetic hydrogel by blending.[19] It can be seen in Figure 2c that, no interface separation between MNPs and chitosan matrix was detected, indicating excellent wettability between *in-situ* synthesized MNPs and chitosan.

XPS spectra were used to clarify the mechanism of MCH formation and the interaction between chitosan and magnetite nanoparticles. The binding energies of N1s were shown in Figure 2e. The binding energy of N1s at 397.8 eV in chitosan attributed to "free" amino group (-NH_2). However, this binding energy disappeared in mixture of iron ions and chitosan, which means that free amino groups disappear. A new binding energy expressed at 401.1 eV, which was attributed to the chelation effect between iron ions and chitosan (-NH_2-Fe(III,II)). After the formation of MCH, the chelation effect disappeared and no free amino groups bond was shown, which meant a weak interaction between amino groups of chitosan and magnetite nanoparticles (-NH_2---Fe_3O_4) was formed. The binding energies of O1s were shown in Figure 2f. It can been that hydroxyl groups of chitosan were also involved in chelation effect (-OH-Fe(III,II)).

The above chelation effect induced homogeneous distribution of MNPs in MCH, and the weak interaction between chitosan and MNPs will enhance the mechanical properties of MCH.

Mechanical Properties of Magnetic Chitosan Hydrogels.

To demonstrate the physical crosslinking effect of *in-situ* synthesized MNPs in MCH, we assessed the mechanical properties of MCH with different magnetite concentrations (0, 5 wt.%, 10 wt.%, 15 wt.% and 20 wt.%). The mechanical properties of MCH were shown in **Figure 3** and **Table 1**. It can be seen from Figure 3a and Table 1 that chitosan hydrogel shows compression strength of 41.6±0.8 kPa, which is 1.86 times stronger than that of hydroxypropyl methyl cellulose gel with same polymer concentration.[28] Moreover, the mechanical properties of MCH were improved significantly (from 41.6±0.8 kPa to 88.6±4.9 kPa) when 5 wt.% *in-situ* synthesized MNPs were involved. The mechanical properties reinforcement of MCH demonstrated a physical crosslinking effect of MNPs on chitosan hydrogel.

When the content of *in-situ* synthesized MNPs increased to 10 wt.% and 15 wt.%, the compression strength and yield strength increased, and the probe displacement when rupture occurred also increased. It can be seen that the mechanical properties of MCH enhanced with the increase of nanoparticles contents (from 0 to 15 wt.%). However, when 20 wt.% MNPs were involved, the compression strength and yield strength increased, but the probe displacement decreased from 14.1 to 12.2 when rupture occurred. The tensile property of MCH with 20 wt.% MNPs can be seen in **Figure S1** (see **Supporting Information**). The above trends can be explained as follows. MNPs act as physical crosslinking points in MCH, which enhanced the strength of hydrogel. However, when an excess of MNPs were introduced, redundant crosslinking points decreased the number of chitosan chains which have interaction with nanoparticles and weakened the crosslinking effect.

Based on the mechanical results of Table 1, the yield strength and elastic modulus of MCH were calculated by **Eq. (1) and (2)**.

$$Yield\ \ strength = (\frac{Yield\ \ force}{1000} \times g) \Big/ \pi r^2 \tag{1}$$

$$Elastic\quad modulus = \frac{Yield\ \ strength}{(Probe\ displacement)/h} \tag{2}$$

where g is acceleration of gravity (g=9.8), r is the radius of probe (r=0.0025m), h is the height of samples (h=40mm).

The yield strength and elastic modulus of MCH are shown in Figure 3b. Chitosan hydrogel shows durable mechanical properties with compress strength of 95.1±7.6 kPa and elastic modulus of 0.46±0.09 MPa. The yield strength increased as high as 416 % (from 95.1±7.6 kPa to 490.9±24.2 kPa) and elastic modulus increased by 265 % (from 0.46±0.09 MPa to 1.68±0.06 MPa) when MNPs were incorporated. However, the strength and modulus of the magnetic alginate hydrogel with chemical crosslinking were only 55 kPa and 30 kPa, respective.[29] The mechanical properties reinforcement demonstrated a physical crosslinking effect of *in-situ* synthesized MNPs on chitosan hydrogel. With the increase of MNPs content (from 5 wt.% to 20 wt.%), a slight increase of yield strength was expressed, and a decrease of elastic modulus was shown (Figure 3b). Similar physical crosslinking effect of hydrogel induced by MNPs has also been reported. The improvements in mechanical properties of hydrogel by addition of nanoparticles depend upon interfacial interaction between nanoparticles and host polymer and state of nanoparticles dispersion. The tight interface of MNPs/chitosan contributes as the physical crosslinking points for hydrogel network (**Figure 1**b).

Passive Drug Release of MCH in Absence of Magnetic Field.

To accurately modulate the entire release profile, it is necessary to clarify the mechanisms that controlled drug release from MCH. For this, we investigated the cumulative release of ADM and RFP from MCH as a function of time. We observed that 40 % percent of ADM was released

within 2 h and the release still sustained after 4 h (**Figure 4**a). We also observed similar release behavior for RFP (Figure 4b), where almost 60 % percent of RFP was released within 60 h and the release continued after 100 h. The release profiles indicated that chitosan hydrogel can be used as continuous drug release for both hydrophilic and hydrophobic drugs. The release of RFP is much slower than that of ADM which is due to that the solubility of RFP (2.5 mg/mL) was smaller than ADM (10 mg/mL). Moreover, the higher molecular weight might, to a certain extent, decrease the diffusion coefficient of RFP.

The release profiles were fitted by four models (Zero-order, First-order, Higuchi and Dissolution-Diffusion model) and the fitted results were shown in **Table 2**. It indicated that zero-order and first-order are not involved in drug release from MCH. If the release profiles of ADM and RFP were fitted by Higuchi model, the correlation coefficients were 88.9 % and 92.5 %, respectively, which suggested that diffusion is the main mechanism of drug release from MCH system.[30] Dissolution-diffusion model assumes that both dissolution and diffusion have effect on the release. In dissolution-diffusion model, the constants k_4 related to diffusion, k_1 related to swelling, k_2 and k_3 related to dissolution. As can be seen from Table 2, the release profiles was best characterized by dissolution-diffusion model with the correlation coefficients 98.6 % and 99.0 %, respectively. The drugs release from MCH in absence of magnetic field is mainly controlled by diffusion. Moreover, the swelling and dissolution related constants (k_1, k_2 and k_3) were very small compared with k_4, which meant that swelling and dissolution of MCH has a little effect on drug release from MCH.

Pulsatile Drug Release of MCH Stimulated by Magnetic Field.

It has been proved that high frequency alternating magnetic field (HAMF) has potential health risks to biological tissue due to the potential heat generation by Neel and Brownian relaxation.[31]

When HAMF at a frequency of 100-500 kHz is used, the temperature of magnetic hydrogel will increase, which in turn enhances the diffusion coefficient D ($D = D_0 e^{-Q/RT}$) of drugs and accelerates drug release. It is impossible to discuss the drug release mechanism under HAMF without the disturbing of heat effect on diffusion coefficient D. Besides, LAMF (specifically, 60 Hz fields) has been conclusively linked to a small number of health effects.[32,33] However, LAMF has no significant heat effect on magnetic hydrogel, which makes it suitable to investigate pure magnetic field stimulated drug release. Hence, LAMF is feasible for remote and noninvasive modulation of drug release from MCH, which can avoid disturbing the stable physiological environment. No temperature change has been detected during drug release when using LAMF (Figure S2, Supporting Information).

The magnetic property of MCH with 20 wt.% MNPs was shown in **Figure 5**. The saturated magnetization (M_s) of MCH reached 10.4 emu/g, which indicated that the M_s of MNPs was 51.2 emu/g. The remanence (M_r) and the coercivity (H_c) were 0.72 emu/g and 14.1 Oe, which proved the superparamagnetic property of MNPs. The above significant magnetization endows MCH with magnetic field responsibility for drug release.

To demonstrate the stimulated effect of LAMF intuitively, we used the LAMF as stimulator and measured the cumulative release of ADM and RFP from hydrogel without or with a LAMF (**Figure 6**). We observed Fickian release for the case without LAMF (Figure 6a and 6b), where the release rate decreased over time. The drug release is passive due to pure diffusion model. However, when a LAMF with 15min ON-15min OFF cycles was applied, the cumulative release was significantly improved. Using LAMF for 1 h, the cumulative release percentage of ADM increased by 67.2 % (from 37.5 % to 62.6 %). Moreover, the release profiles of Figure 6 were

fitted by Zero-order model, and the fitted results indicated that the drug release rate related slope K_0 increase from 20.80 to 40.56 when LAMF was used (Figure S3, Supporting Information).

The fraction release profiles of ADM were shown in Figure 6c, LAMF can switch the speed of drug release from passive release to pulsatile release with quick response. Without magnetic stimulation, the fraction release percentage of ADM was 11.3 % (0~0.25h region) and 8.4 % (0.25h~0.5h region), respectively (Figure 6c). A decrease of fraction release by 37 % was observed. However, when low frequency magnetic field stimulation was applied, the fraction release increased (Figure 6d). During the 0~0.25h region (magnetic OFF), a fraction release percentage 11.3 % was given, same as Figure 6c. During the 0.25~0.5h region (magnetic ON), a fraction release percentage 14.9 % was given, which is almost twice of Fickian fraction release rate. As the 15min ON-15min OFF cycles was applied, a pulsatile release with quick response profile was generated. Fraction release profiles of insoluble RFP from MCH were plotted in Figure 6e and Figure 6f. Similar observations as ADM were observed. Without magnetic field stimulation, the fraction release percentage of RFP slightly decreased (Figure 6e). The applied magnetic field stimulation greatly accelerated the release of FRP. When magnetic field stimulation was applied, a correspondence increase of fraction release was given (Figure 6f). Comparing 0~1h region (magnetic OFF) and 1~2h region (magnetic ON), the fraction release percentage increased by 39.3 %. The cumulative release profile showed a quick increment with magnetic stimulation, and the total amount of drug released from the stimulated gel was 39.9 % faster than that of the control group. Moreover, paired samples *t* test was used to identify with significant differences between LAMF drug release and passive drug release. Statistically significant differences were observed between LAMF drug release and passive drug release (Figure 6a and 6b; p values were 0.028 and 0.006 for ADM and RFP, respectively).

The magnetic remotely controlled drug release offered distinct clinical advantages over passively release or other stimulation. For example, clinical doctors can facile upload single or multiple anti-infective drugs in MCH during the operation, the magnetic field stimulation pulsatile release can modulate the drug release dose to terminate surgical infection. The principle of LAMF on release properties of MCH is illustrated in Figure 1c. Without LAMF, the drug release profiles are passive due to diffusion controlled model. However, significant magnetization was shown by the superparamagnetic nanoparticles under the LAMF, which induced deformation of MCH (weight decreased 8.5 % under static magnetic field, see Figure S4 in Supporting Information), and subsequent allowed promoting faster release of entrapped drug from the MCH. Magnetic field stimulated drug release behavior was attributed to the deformation and resulting water convection of drug carrier.[19]

Cytotoxicity of Magnetite Nanoparticles Released from MCH.

MNPs hold great therapeutic potential, but naked MNPs can be toxic.[24] During degradation of MCH, *in-situ* synthesized MNPs release was unavoidable. To assess of the cytotoxicity of *in-situ* synthesized MNPs, MG-63 cells were cultured with different doses of *in-situ* synthesized MNPs. The MG-63 cell viability was 87 % (as shown in **Figure 7**a) according to the MTT assay, which indicated that the *in-situ* synthesized MNPs from MCH do not express acute toxicity on MG-63 cells even at dosage up to 200 mg/L.

The morphology of MG-63 cells with internalized MNPs was shown in Figure 7. The agglomerates of *in-situ* synthesized MNPs were distributed in cytoplasm of MG-63 (pointed by red arrows). However, no MNPs were detected in the lysosome, golgi organ, mitochondria and nucleus. Several endocytosis mechanisms have been identified, including caveolae, phagocytosis, receptor-mediated endocytosis, clathrin-mediated endocytosis and macropinocytosis. Caveolate

and phagocytosis were not involved for intracellular uptake of *in-situ* synthesized MNPs. The nanoparticles internalized via clathrin-mediated endocytosis or receptor-mediated endocytosis was commonly detected in the intracellular vesicles. The nanoparticles in MG-63 cells were distributed in cytoplasm, which validated that the main endocytosis mechanism is macropinocytosis. Especially, if MNPs were captured by lysosome, the MNPs would be eliminated from the body through lysosomal degradation.[36] The distribution of MNPs in cytoplasm indicated satisfied biocompatibility of MNPs. According to the MTT results and cell morphology after culturing, the *in-situ* synthesized MNPs released from MCH have excellent biocompatibility and no acute adverse effect on MG-63 cells.

Conclusion

Magnetic chitosan hydrogels (MCH) were fabricated via facile *in-situ* hybridization and magnetic field remotely stimulated drug release from MCH was realized. During *in-situ* hybridization, the iron ions were chelated by chitosan, which induced the *in-situ* synthesized MNPs have a significant physical crosslinking effect on MCH. Strength and elastic modulus of MCH was improved as high as 416 % and 265 %, respectively. Both hydrophilic drug ADM and hydrophobic drug RFP release from the hydrogel were mainly controlled by diffusion mechanism. When a low frequency alternating magnetic field (LAMF) was applied to the MCH, the cumulative release of ADM improved by 67.2 % than passive release. When an ON-OFF LAMF was used, the MCH show a sustained drug release as well as modulatory release. If loaded with anti-infected drugs, the continuous drug release of MCH can avoid the infection and the magnetic field stimulation release can terminate it once infection occurs. The *in-situ* synthesized MNPs released from MCH do not express acute toxicity on MG-63 cells even at dosage up to 200 mg/mL. The MCH has potential applications as an implantable drug carrier for

localized drug delivery system in anti-infection bone tissue engineering stimulated by noninvasive low frequency alternating magnetic field.

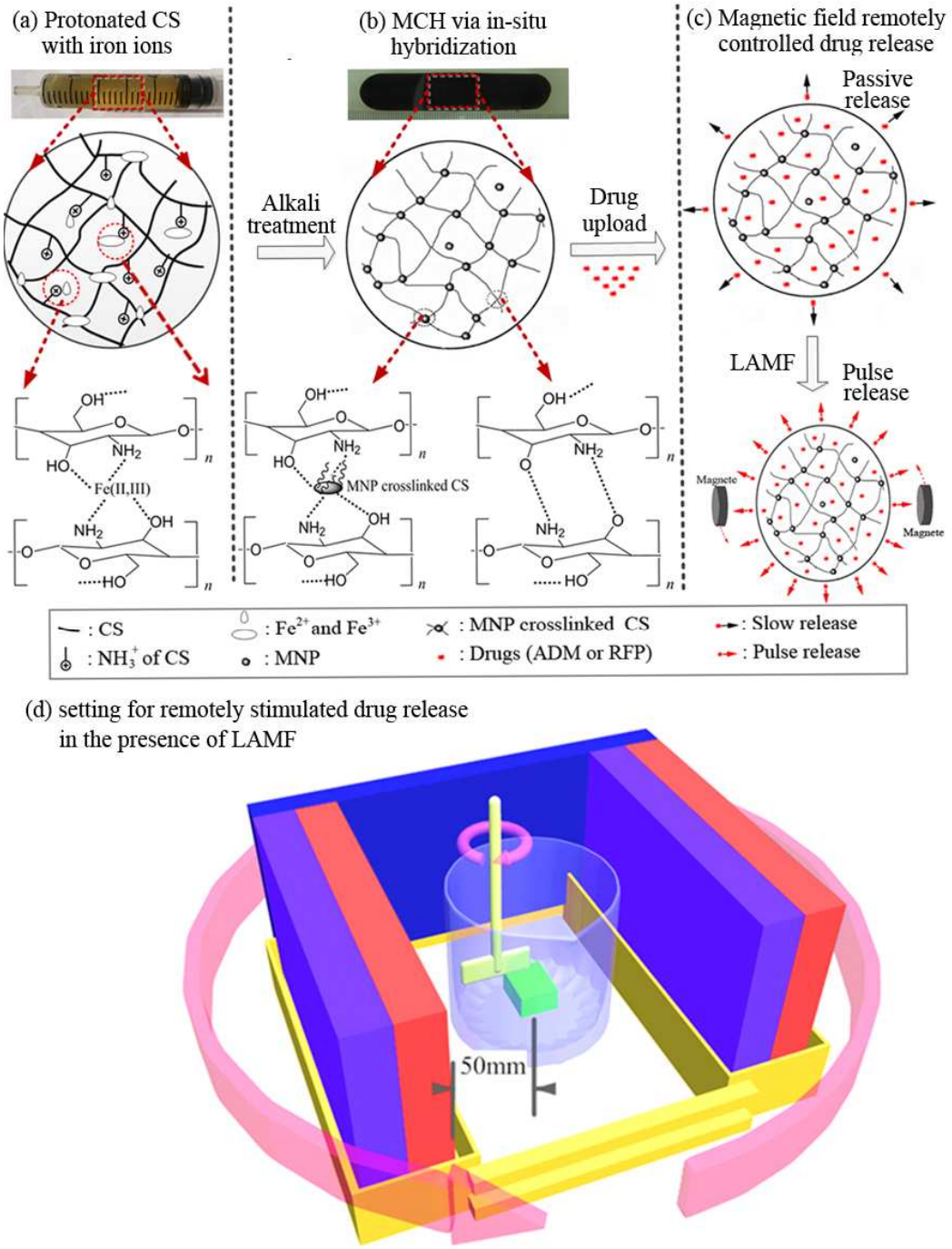

Figure 1. Schematic presentation of the principle of *in-situ* hybridization for MCH (a, b) and low frequency alternating magnetic field (LAMF) remotely stimulated drug release of MCH (c, d).

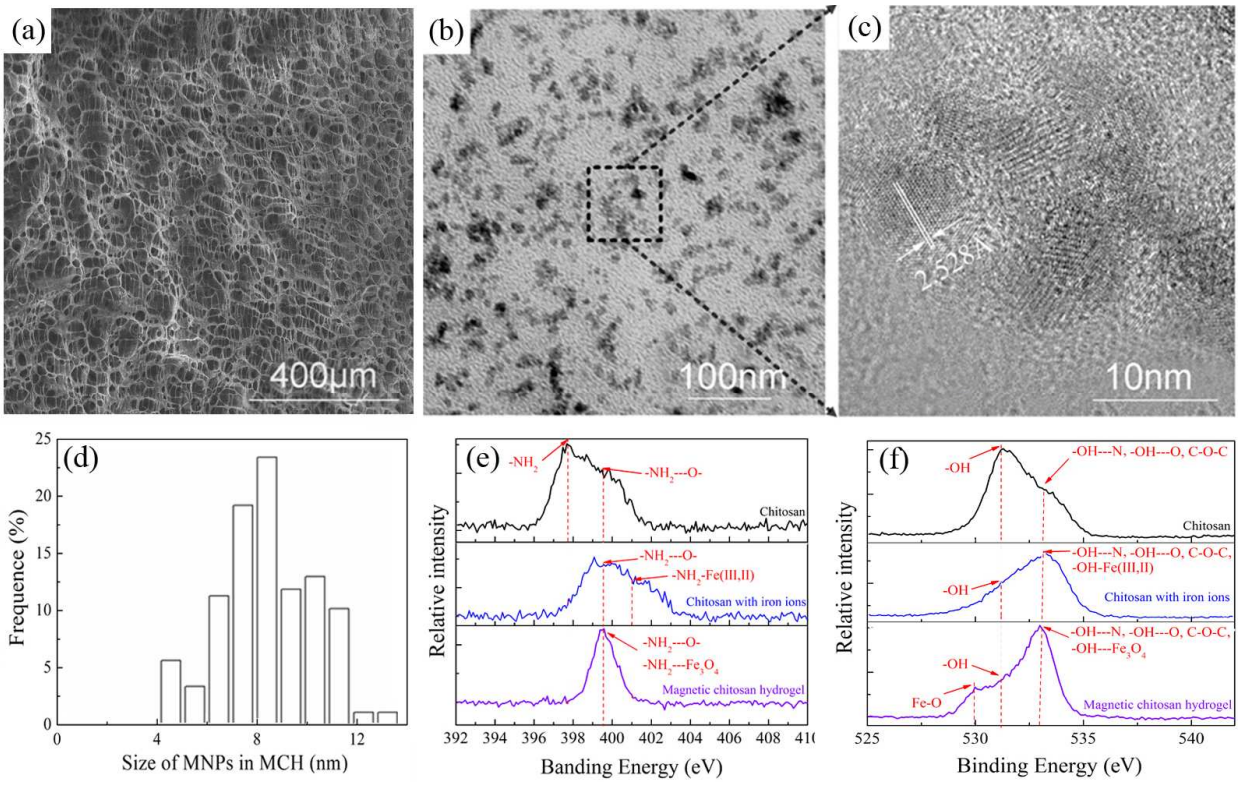

Figure 2. ESEM morphology of MCH (a). TEM and HRTEM images of MNPs in MCH (b, c) and statistic size of MNPs in MCH (d). XPS spectra of N1s (e) and O1s (f) during synthesis of MCH.

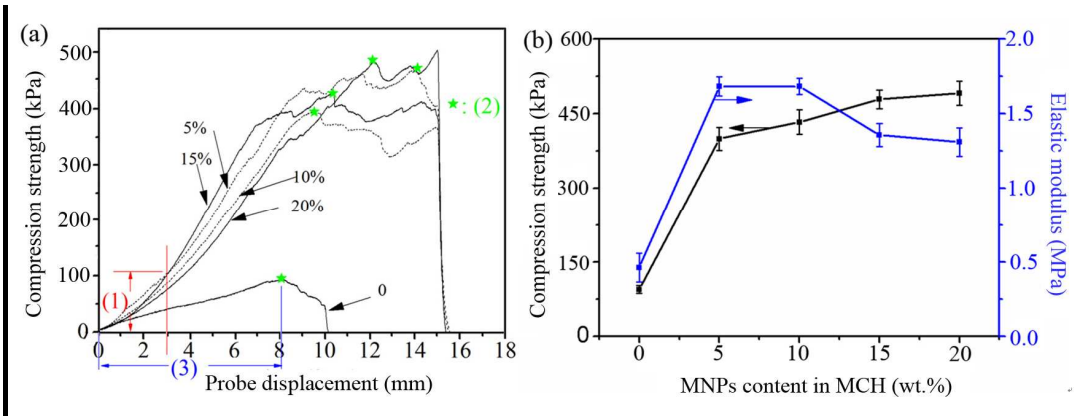

Figure 3. The compression testing profiles of MCH with different magnetite contents (a) and the compression strength and elastic modulus of MCH (b). (Note: (1) The strength that the probe penetrates 3 mm is "compression strength". (2) The maximum strength is indicative of "yield strength". (3) The probe displacement when rupture occurs.)

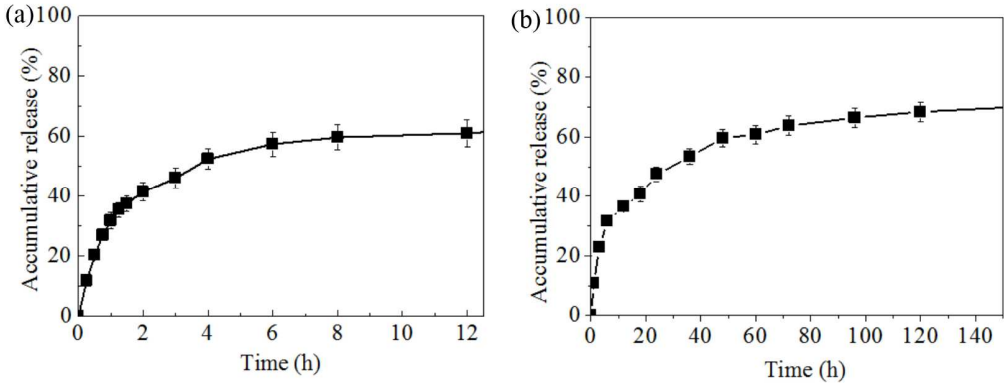

Figure 4. The release profiles of hydrophilic ADM (a) and hydrophobic RFP (b) from MCH.

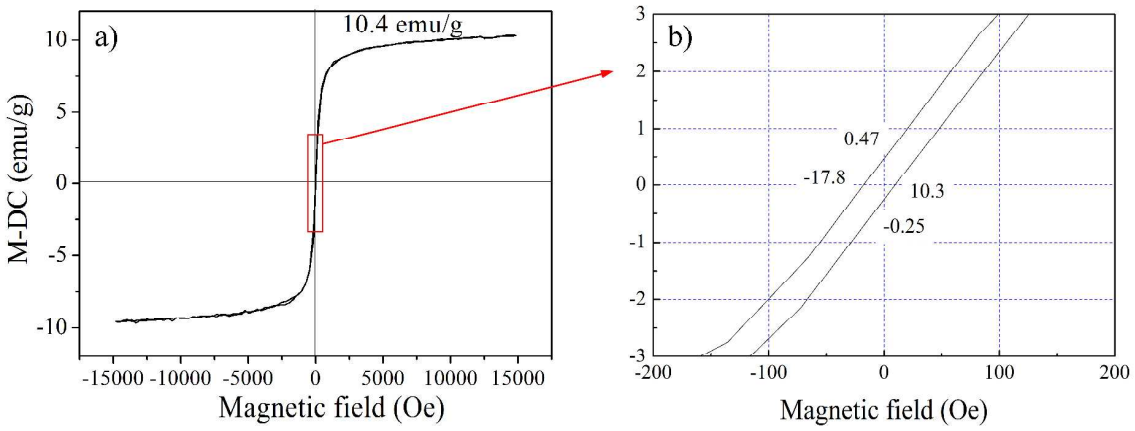

Figure 5. Hysteresis loop of the magnetic chitosan hydrogel at 300 K

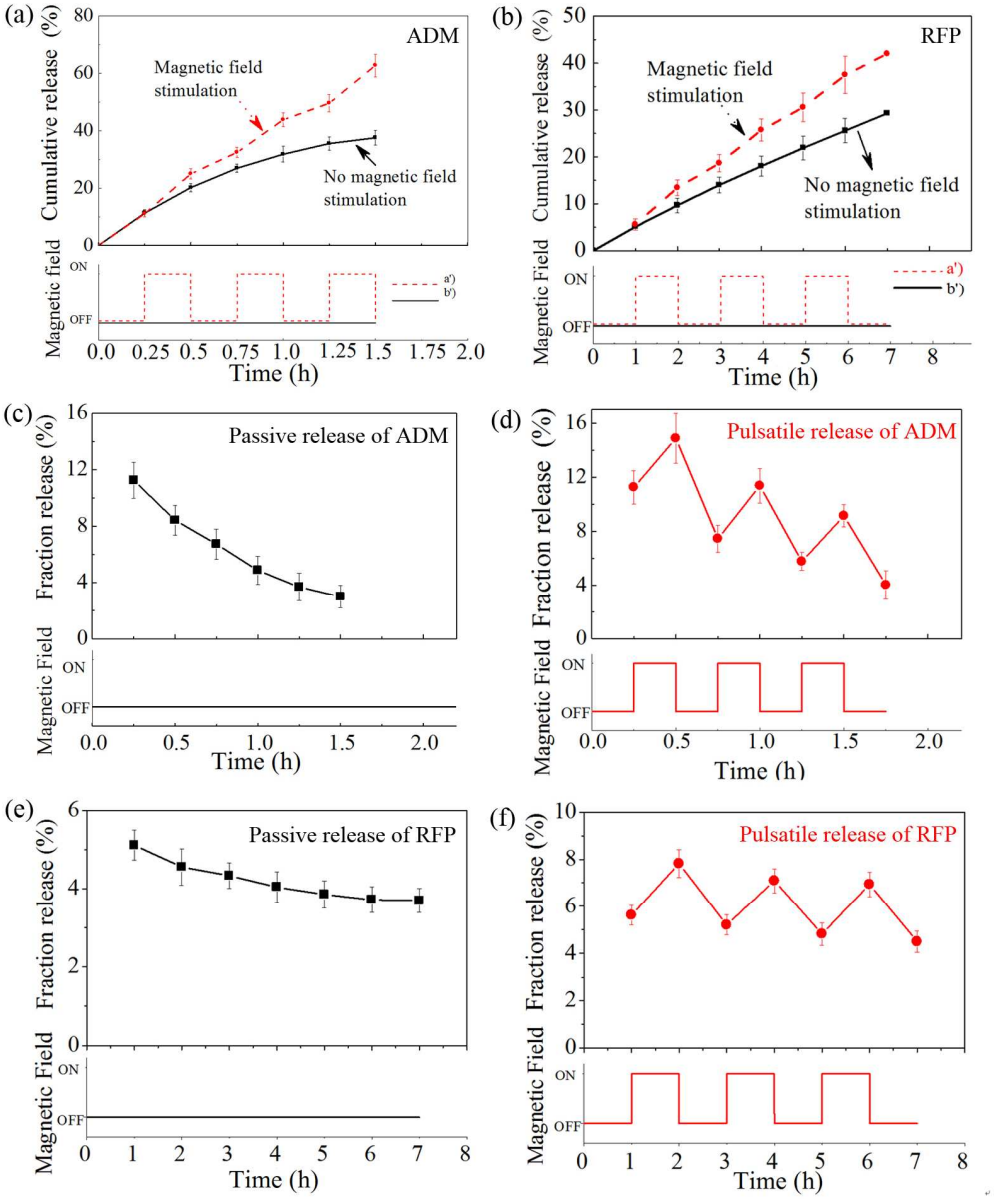

Figure 6. Drug release profiles with and without magnetic field remote stimulation. Cumulate release profiles of hydrophilic ADM (a) and hydrophobic RFP (b) with and without of LAMF. Fraction release profile of ADM in the absence of LAMF (c) and pulsatile release with quick responsive stimulated by LAMF (d). Fraction release profile of RFP in the absence of LAMF (e) and pulsatile release behavior with quick responsive stimulated by LAMF (f).

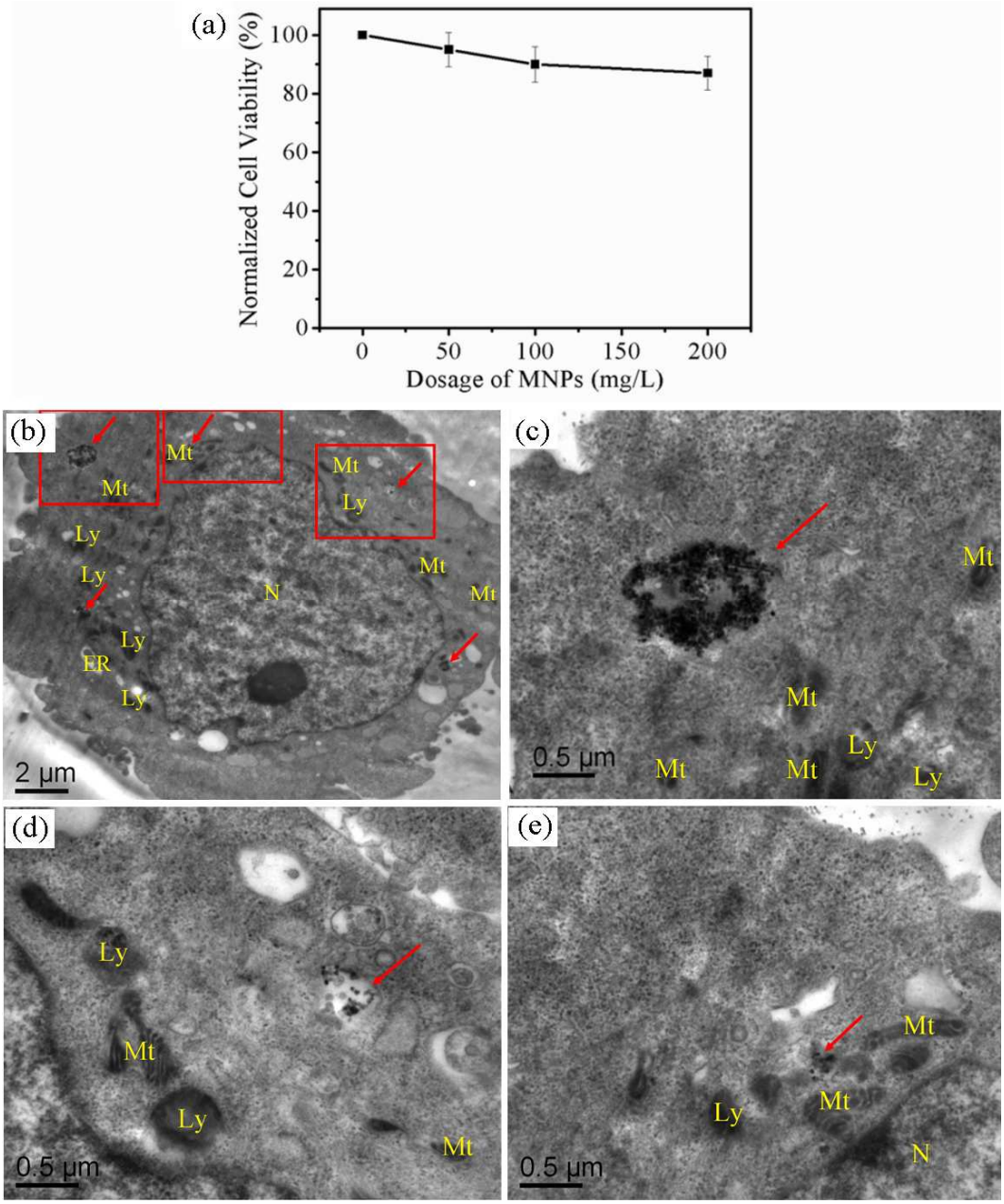

Figure 7. Cell viability dependent on *in-situ* synthesized MNPs dosage (a) and morphologies of MG-63 cells with internalized MNPs released from MCH (b, c, d and e). N, nucleus; Ly, lysosome; Mt, mitochondria; ER, endoplasmic reticulum.

Table 1. The mechanical properties of MCH with different magnetite contents

MNPs content (wt.%)	Compression strength (kPa)	Yield strength (kPa)	Probe displacement (mm)
0	41.6±0.8	95.1±7.6	8.2±0.8
5	88.6±4.9	399.0±11.5	9.5±0.9
10	102.4±5.8	432.5±13.1	10.3±1.0
15	107.9±6.2	477.9±15.1	14.1±1.2
20	76.8±4.3	490.9±24.2	12.2±1.1

Table 2. Fitting results of mathematical for release of ADM or RFP from MCH

Model	Formulation	ADM		RFP	
		Coefficient K	R^2	Coefficient K	R^2
Zero-order	$Q_t = Q_0 + K_0 t$	K_0=2.268	0.745	K_0=0.814	0.732
First-order	$\ln(1-Q) = -Kt$	K=0.073	0.769	K=0.013	0.678
Higuchi	$Q_t = K_H t^{1/2}$	K_H=18.104	0.889	K_H=7.691	0.925
Dissolution-diffusion	$Q_t = k_4 t^{1/2} + k_1 t + k_2 t^2 + k_3 t^3$	k_4=30.241 k_1=0.594 k_2=0.764 k_3=0.034	0.986	k_4=16.020 k_1=-1.513 k_2=0.010 k_3=0	0.990

ASSOCIATED CONTENT

Supporting Information.

The following files are available free of charge.

1. Tough Magnetic Chitosan Hydrogel Nanocomposites for Remotely Stimulated Drug Release (pdf)

AUTHOR INFORMATION

Corresponding Author

*Email: libq@hit.edu.cn (B. Li)

ACKNOWLEDGMENT

B.Q. Li thanks the financial support from National Science Foundation of China (51372051, 51621091), State Key Laboratory of Urban Water Resource and Environment of HIT (2016TS03), HIT Environment and Ecology Innovation Special Funds (HSCJ201623). Y.L. Wang thanks the financial support from National Science Foundation of China (51602084). F. Xu was supported by the Major International Joint Research Program of China (No. 11120101002) and International Science & Technology Cooperation Program of China (No. 2013DFG02930).

REFERENCES

(1) Huang, G.Y.; Li, F.; Zhao, X.; Ma, Y.F.; Li, Y.H.; Lin, M.; Jin, G.R.; Lu, T.J.; Genin, G.; Xu, F., Functional and Biomimetic Materials for Engineering of the Three-Dimensional Cell Microenvironment. *Chem. Rev.* **2017**,117, 12764-12850.

(2) Cánepa, C.; Imperiale, J. C.; Berini, C. A.; Lewicki, M.; Sosnik, A.; Biglione, M. M., Development of a Drug Delivery System based on Chitosan Nanoparticles for Oral Administration of Interferon-α. *Biomacromolecules*, **2017**,18(10), 3302-3309.

(3) Shademani, A.; Zhang, H. B.; Jackson, J. K.; Chiao, M., Active Regulation of On-Demand Drug Delivery by Magnetically Triggerable Microspouters. *Adv. Funct. Mater.* **2017**, 27, 1604558.

(4) Bhattarai, N.; Gunn, J.; Zhang, M., Chitosan-Based Hydrogels for Controlled, Localized Drug Delivery. *Adv. Drug Deliver. Rev.* **2010**, 62, 83-99.

(5) Martínez-Martínez, M.; Rodríguez-Berna, G.; Gonzalez-Alvarez, I.; Hernández, M. J.; Corma, A.; Bermejo, M.; Merino, V.; Gonzalez-Alvarez, M., Ionic Hydrogel Based on Chitosan Cross-Linked with 6-Phosphogluconic Trisodium Salt as a Drug Delivery System. *Biomacromolecules*, **2018**, 19(4), 1294-1304.

(6) Chen, C. K.; Huang, S. C., Preparation of Reductant-Responsive N-Maleoyl-Functional Chitosan/Poly(vinyl alcohol) Nanofibers for Drug Delivery. *Mol.Pharmaceutics*, **2016**, 13(12), 4152-4167.

(7) Amoozgar, Z.; Park, J.; Lin, Q.; Yeo, Y., Low Molecular-Weight Chitosan as a pH-Sensitive Stealth Coating for Tumor-Specific Drug Delivery. *Mol. Pharm.* **2012**, 9, 1262-1270.

(8) Dong, Y. Y.; Kim, J. C., Hydrogel Composed of Acrylic Coumarin and Acrylic Pluronic F-127 and its Photo- and Thermo-Responsive Release Property. *Biotechnol. Bioprocess Eng.* **2017**, 22(4), 481-488.

(9) Skaalure, S. C.; Akalp, U.; Vernerey, F. J.; Bryant, S. J., Tuning Reaction and Diffusion Mediated Degradation of Enzyme-Sensitive Hydrogels. *Adv. Healthc. Mater.* **2016**, 5(4), 432-438.

(10) Agarwal, A.; Mackey, M. A.; Elsayed, M. A.; Bellamkonda, R. V., Remote Triggered Release of Doxorubicin in Tumors by Synergistic Application of Thermosensitive Liposomes and Gold Nanorods. *Acs Nano* **2011**, 5, 4919-4926.

(11) Jahren, S. L.; Butler, M. F.; Adams, S.; Cameron, R. E.; Swelling and Viscoelastic Characterisation of pH-Responsive Chitosan Hydrogels for Targeted Drug Delivery. *Macromol. Chem. Phys.* **2010**, 211(6), 644-650.

(12) Zhao, X.; Kim, J.; Cezar, C. A.; Huebsch, N.; Lee, K.; Bouhadir, K., Active Scaffolds for on-Demand Drug and Cell Delivery. P. Natl. Acad. Sci. USA **2011**, 108(1), 67-72.

(13) Moghanjoughi A. A.; Khoshnevis, D.; Zarrabi, A., A Concise Review on Smart Polymers for Controlled Drug Release. *Drug Deliv. Transl. Res.* **2016**, 6(3), 1-8.

(14) Xu, F.; Wu, C. A.; Rengarajan, V.; Finley, T. D.; Keles, H. O.; Sung, Y., Three-Dimensional Magnetic Assembly of Microscale Hydrogels. *Adv. Mater.* **2011**, 23(37), 4254-4260.

(15) Haider, H.; Yang, C. H.; Zheng, W. J.; Yang, J. H.; Wang, M. X.; Yang, S.; Zrinyi, M.; Osada Y.; Suo, Z. G.; Zhang, Q. Q.; Zhou, J. X.; Chen, Y. M., Exceptionally Tough and Notch-Insensitive Magnetic Hydrogels. *Soft Matter.* **2015**, 11(42), 8253-8261.

(16) Bakalova, R.; Nikolova, B.; Murayama, S.; Atanasova, S.; Zhelev, Z.; Aoki, I., Passive and Electro-Assisted Delivery of Hydrogel Nanoparticles in Solid Tumors, Visualized by Optical and Magnetic Resonance Imaging in vivo. *Anal. Bioanal. Chem.* **2016**, 408, 905-914.

(17) Namdari, M.; Eatemadi, A., Cardioprotective Effects of Curcumin-Loaded Magnetic Hydrogel Nanocomposite (Nanocurcumin) Against Doxorubicin-Induced Cardiac Toxicity in Rat Cardiomyocyte Cell Lines. *Artif. Cell Nanomed. B* **2016**, 45(4), 731-739.

(18) Rodkate, N.; Rutnakornpituk, M., Multi-Responsive Magnetic mMicrosphere of Poly(N-isopropylacrylamide)/Carboxymethyl Chitosan Hydrogel for Drug Controlled Release. *Carbohyd. Polym.* **2016**, 151, 251-259.

(19) Xu, F.; Inci, F.; Mullick, O.; Gurkan, U. A.; Sung, Y.; Kavaz, D., Release of Magnetic Nanoparticles from Cell-Encapsulating Biodegradable Nanobiomaterials. *Acs Nano* **2012**, 6(8), 6640-6649.

(20) Vikingsson, L.; Vinals-Guitart, A.; Valera-Martínez, A.; Riera, J.; Vidaurre, A.; Ferrer, G. G., Local Deformation in a Hydrogel induced by an External Magnetic Field. *J. Mater. Sci.* **2016**, 51(22), 1-12.

(21) Zivpolat, O.; Skaat, H.; Shahar, A.; Margel, S., Novel Magnetic Fibrin Hydrogel Scaffolds Containing Thrombin and Growth Factors Conjugated Iron Oxide Nanoparticles for Tissue Engineering. *Inter. J. Nanomed.* **2012**, 7, 1259-1274.

(22) Ray, C. A.; Singh, T.; Ghosh, S. K.; Sahu, S. K., Carbon Dots Embedded Magnetic Nanoparticles@Chitosan@Metal Organic Framework as a Nanoprobe for pH Sensitive Targeted Anticancer Drug Delivery. *ACS Appl. Mater Inter*, **2016**, 8(26), 16573-16583.

(23) Pour, Z. S.; Ghaemy, M.; Removal of Dyes and Heavy Metal Ions from Water by Magnetic Hydrogel Beads based on Poly(vinyl alcohol)/Carboxymetyl Starch-g-poly(vinyl imidazole). *Rsc Adv.* **2015**, 5(79), 64106-64118.

(24) Agotegaray, M. A.; Campelo, A. E.; Zysler, R. D.; Gumilar, F.; Bras, C.; Gandini, A., Magnetic Nanoparticles for Drug Targeting: from Design to Insights into Systemic Toxicity. Preclinical Evaluation of Hematological, Vascular and Neurobehavioral Toxicology. *Biomater. Sci.* **2017**, 5, 772-783.

(25) Zhao, S. H.; Lin, X. L.; Zhang, L.; Sun, L.; Li, J.; Yang, W. S., The in Vivo Investigation of Fe_3O_4-Nanoparticles Acute Toxicity in Mice. *Biomed. Eng.-App. Basis C* **2012**, 24(3), 229-235.

(26) González-Alfaro, Y.; Aranda, P.; Fernandes, F. M.; Wicklein, B.; Darder, M.; Ruiz-Hitzky, E., Multifunctional Porous Materials Through Ferrofluids. *Adv. Mater.* **2011**, 23(44), 5224-5228.

(27) Varga, Z.; Filipcsei, G.; Zrínyi, M., Magnetic Field Sensitive Functional Elastomers with Tuneable Elastic Modulus. *Polymer* **2006**, 47(1), 227-233.

(28) Dhawan, S.; Medhi, B.; Chopra, S., Formulation and Evaluation of Diltiazem Hydrochloride Gels for the Treatment of Anal Fissures. *Sci. Pharm.* **2009**, 77, 465-482.

(29) Huang, T.; Xu, H. G.; Jiao, K. X.; Zhu, L. P.; Brown, H. R.; Wang, H. L., A Novel Hydrogel with High Mechanical Strength: A Macromolecular Microsphere Composite Hydrogel. *Adv. Mater.* **2007**, 19, 1622-1626.

(30) Mahdavinia, G. R.; Mosallanezhad, A.; Soleymani, M.; Sabzi, M., Magnetic- and pH-Responsive k-Carrageenan/Chitosan Complexes for Controlled Release of Methotrexate Anticancer Drug. *Int. J. Biol. Macromol.* **2017**, 97, 209-217.

(31) Brulé, S.; Levy, M.; Wilhelm, C.; Letourneur, D.; Gazeau, F.; Ménager, C., Doxorubicin Release Triggered by Alginate Embedded Magnetic Nanoheaters: A CombinedTherapy. *Adv. Mater.* **2011**, 23, 787-790.

(32) Lai, H C; Singh, N. P., Medical Applications of Electromagnetic Fields[C]// IOP Conference Series: Earth and Environmental Science. IOP Conference Series: Earth and Environmental Science, **2010**:012006.

(33) Joseph, K.; Jackie, W.; Robert, L., Magnetically Enhanced Insulin Release in Diabetic Rats. *J. Biomed. Mater. Res.* **1987**, 21(12), 1367-1373.

(34) Wang, Y. L.; Li, B. Q.; Zhou, Y.; Jia, D. C.; Song, Y., CS-Fe(II,III) Complex as Precursor for Magnetite Nanocrystal. *Polym. Adv. Technol.* **2011**, 22, 1681-1684.

(35) Singh, B.; Pal, L., Sterculia Crosslinked PVA and PVA-poly(AAm) Hydrogel Wound Dressings for Slow Drug Delivery: Mechanical, Mucoadhesive, Biocompatible and Permeability Properties. *J. Mech. Behav. Biomed.* **2012**, 9, 9-21.

(36) Liu, P. F.; Sun, Y. M.; Wang, Q.; Sun, Y.; Li, H.; Duan, Y. R., Intracellular trafficking and cellular uptake mechanism of mPEG-PLGA-PLL and mPEG-PLGA-PLL-Gal nanoparticles for targeted delivery to hepatomas. *Biomaterials,* **2014**, 35, 760-770.

Toc/Abstract graphic

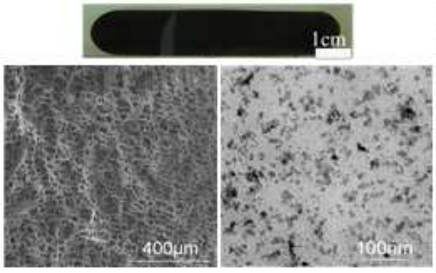

Tough magnetic chitosan hydrogel reinforced by physical crosslinking of *in-situ* synthesized MNPs

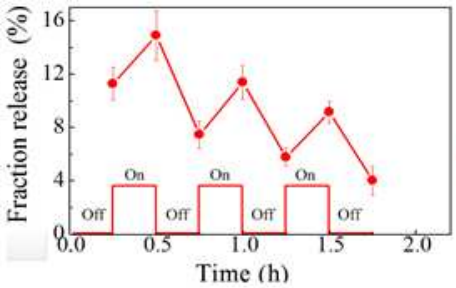

Remotely tailor-made pulsatile release profile for **smart** localized drug release to match the biological rhythm for blood drug concentration.